Bioorganic & Medicinal Chemistry xxx (2016) xxx–xxx

Contents lists available at ScienceDirect

Bioorganic & Medicinal Chemistry

journal homepage: www.elsevier.com/locate/bmc

Discovery of potent anti-tuberculosis agents targeting leucyl-tRNA synthetase

Olga I. Gudzera [a], Andriy G. Golub [b], Volodymyr G. Bdzhola [a], Galyna P. Volynets [a], Sergiy S. Lukashov [a], Oksana P. Kovalenko [a], Ivan A. Kriklivyi [a], Anna D. Yaremchuk [a], Sergiy A. Starosyla [a], Sergiy M. Yarmoluk [a,*], Michail A. Tukalo [a]

[a] Institute of Molecular Biology and Genetics, NAS of Ukraine, 150 Zabolotnogo St., 03680 Kyiv, Ukraine
[b] OTAVA Ltd, 400 Applewood Crescent, Unit 100, Vaughan, Ontario L4K0C3, Canada

ARTICLE INFO

Article history:
Received 5 October 2015
Revised 23 December 2015
Accepted 15 January 2016
Available online xxxx

Keywords:
Mycobacterium tuberculosis
Leucyl-tRNA synthetase
Inhibitor
Virtual screening
Aminoacylation assay

ABSTRACT

Tuberculosis is a serious infectious disease caused by human pathogen bacteria *Mycobacterium tuberculosis*. Bacterial drug resistance is a very significant medical problem nowadays and development of novel antibiotics with different mechanisms of action is an important goal of modern medical science. Leucyl-tRNA synthetase (LeuRS) has been recently clinically validated as antimicrobial target. Here we report the discovery of small-molecule inhibitors of *M. tuberculosis* LeuRS. Using receptor-based virtual screening we have identified six inhibitors of *M. tuberculosis* LeuRS from two different chemical classes. The most active compound 4-{[4-(4-Bromo-phenyl)-thiazol-2-yl]hydrazonomethyl}-2-methoxy-6-nitro-phenol (**1**) inhibits LeuRS with IC_{50} of 6 μM. A series of derivatives has been synthesized and evaluated in vitro toward *M. tuberculosis* LeuRS. It was revealed that the most active compound 2,6-Dibromo-4-{[4-(4-nitro-phenyl)-thiazol-2-yl]-hydrazonomethyl}-phenol inhibits LeuRS with IC_{50} of 2.27 μM. All active compounds were tested for antimicrobial effect against *M. tuberculosis* H37Rv. The compound **1** seems to have the best cell permeability and inhibits growth of pathogenic bacteria with IC_{50} = 10.01 μM and IC_{90} = 13.53 μM.

1. Introduction

Tuberculosis is one of the world's deadliest diseases and a serious public health problem. A major problem of tuberculosis treatment is increasing resistance to antibiotics. This provides the stimulus for search of novel antibiotics with different mechanisms of action. The inhibition of bacterial protein synthesis represents ideal target for drug discovery. Aminoacyl-tRNA synthetases (aaRSs) play an indispensable role in protein synthesis and their structures have some differences in prokaryotes and eukaryotes.[1,2] This structural divergence can be exploited for the development of drugs that inhibit a pathogen synthetase but not its human cell counterpart. It is known that substitution of key amino acid residues in the enzyme active site leads to the drug resistance. Since aaRSs don't mutate very easily these enzymes are less likely to become drug-resistant. Therefore, aaRSs are reported to be promising drug targets.[3–6]

At present time it is known several mechanisms of aaRSs inhibition. Most inhibitors interact with the highly conservative synthetic active site and act as amino acid competitive inhibitors or mimic aminoacyl-adenylate. Among the inhibitors which compete with amino acids, there were reported analogs of isoleucine such as cispentacin[7] and icofungipen,[8] tryptophan analog—indolmycin,[9] proline analog—halofuginone,[10] phenylalanine analog—ochratoxin A.[11] A substantial number of inhibitors mimic aminoacyl-adenylate. For example, mupirocin (pseudomonic acid) is a natural inhibitor of isoleucyl-tRNA synthetase (IleRS) from gram-positive bacteria.[12] There were designed a number of synthetic inhibitors which compete with aminoacyl-adenylate with nanomolar and picomolar affinities toward aaRSs.[13–17] Also, a number of inhibitors bind to other regions of the aaRSs outside the active site, either allosterically affecting the synthetic active site or binding to alternative active sites, such as the editing domain.[18,19]

LeuRS plays an essential role in cellular translation and recently has been clinically validated as antimicrobial target. Earlier, the inhibitor of LeuRS—AN2690, was proposed as a new class of antifungal agent for the topical treatment of onychomycosis.[18] Recently, there were published inhibitors of *Streptococcus pneumonia*[20] and *Trypanosoma brucei* LeuRS.[14,15,21] However, to the best

Abbreviations: LeuRS, leucyl-tRNA synthetase; aaRSs, aminoacyl-tRNA synthetases; IleRS, isoleucyl-tRNA synthetase.

* Corresponding author. Tel.: +38 044 522 2458; fax: +38 044 200 0335.
E-mail address: sergiy@yarmoluk.org.ua (S.M. Yarmoluk).

http://dx.doi.org/10.1016/j.bmc.2016.01.028
0968-0896/

of our knowledge none of the small molecule inhibitors of *Mycobacterium tuberculosis* LeuRS have been reported in scientific literature so far. Therefore, the main aim of this research is to identify the small molecule inhibitors of *M. tuberculosis* LeuRS.

2. Results and discussion

In order to discover inhibitors of *M. tuberculosis* LeuRS we have performed screening program, using computer modeling methods and in vitro approaches. The system based on DOCK package was applied to perform receptor–ligand flexible docking.[22–25] The three dimensional structure of *M. tuberculosis* LeuRS was modeled using the known *Thermus thermophilus* LeuRS structure as a template.[18,26] Amino acid sequence identity of the full length *M. tuberculosis* LeuRS and *T. thermophilus* LeuRS is 37%. However, the synthetic active sites of two enzymes share about 95% sequence homology. Therefore, the *M. tuberculosis* LeuRS synthetic active site should serve as a quite acceptable model for the following virtual screening.

We have performed pairwise alignment of amino acid sequences for *M. tuberculosis* and human LeuRS using ClustalW program. It was revealed that these two enzymes have significant difference in the amino acid sequences of their active sites (Fig. 1). This structural divergence can be basis for development of inhibitors with selective action toward *M. tuberculosis* LeuRS.

In this study the virtual screening experiments were carried out targeting the active site of *M. tuberculosis* LeuRS by screening the compound library of 100,000 organic compounds. After the docking followed by visual inspection of the best-scored complexes having score less than −40 kcal/mol, 270 compounds were selected for biochemical testing of their inhibitory activity toward *M. tuberculosis* LeuRS. In vitro experiments revealed that six compounds from two different chemical classes demonstrated inhibitory activity toward *M. tuberculosis* LeuRS (Table 1).

Several important structural features of these compounds can be identified from analysis of their activity on LeuRS *M. tuberculosis*.

Compounds **1**, **2**, **3** and **4** belong to the one chemical class—derivatives of *N*-Benzylidene-*N*′-thiazol-2-yl-hydrazine. Interestingly, other compounds with 4-thiazolidinon core have been found to have anti-tubercular activity.[27,28]

Compounds **1** and **2** differ from each other by the nature of substituent at the fourth position in the benzene ring which accordingly to binding mode obtained with molecular docking interacts with amino acid residues Tyr99, Trp628, Ser631, His681 and His685 in the adenine-binding region (Fig. 2). A substitution of bromine atom (compound **1**) with a nitro group (compound **2**) results in slightly decreasing of inhibitory activity (IC_{50} = 6 and 8 μM, respectively). Apparently, it can be caused by the ability of bromine

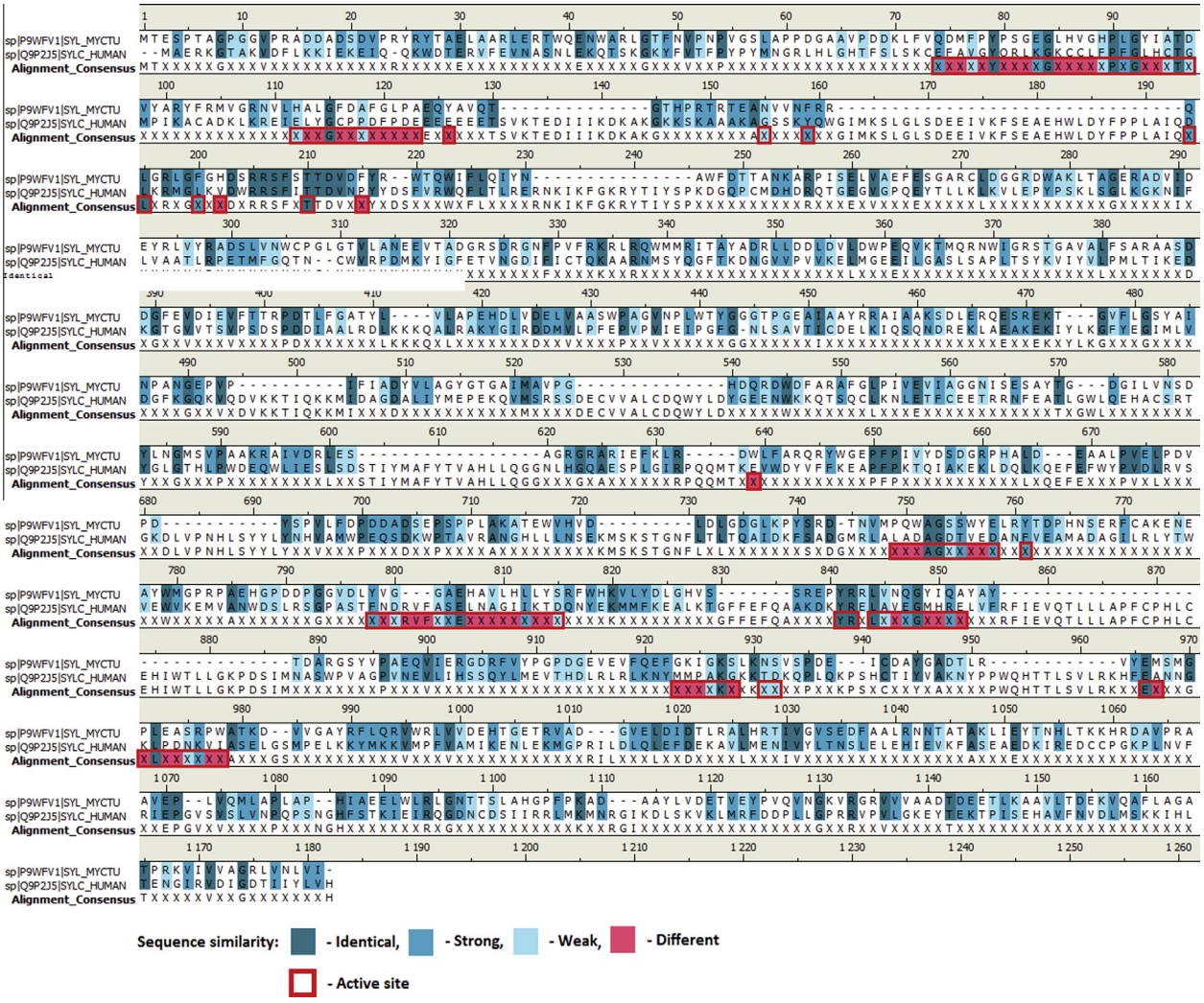

Figure 1. Alignment of amino acid sequences for *M. tuberculosis* and human LeuRS.

Table 1
Compounds chemical structure and in vitro inhibitory activity toward *M. tuberculosis* leucyl-tRNA synthetase

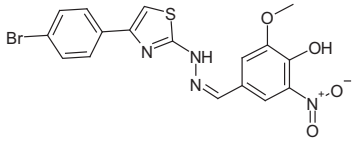 Compound **1** (IC_{50} = 6 μM)	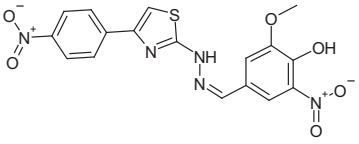 Compound **2** (IC_{50} = 8 μM)
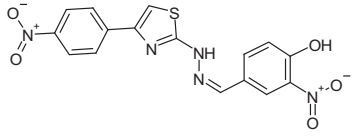 Compound **3** (IC_{50} = 20 μM)	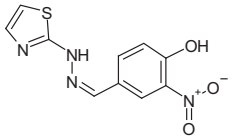 Compound **4** (IC_{50} = 20 μM)
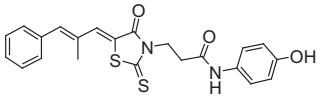 Compound **5** (IC_{50} = 22.2 μM)	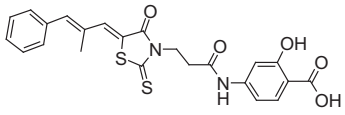 Compound **6** (IC_{50} > 50 μM)

atom to form hydrophobic interactions with the amino acid residues in adenine-binding region.

The LeuRS inhibitory activity of compounds in this class depends on the chemical structure of substituents on another benzene ring which accordingly to computer simulation, interacts with amino acid residues Gly108, His109, Leu111, Gly112, Gln714, Gly715, Tyr716 and Ile717 in leucyl-binding region of LeuRS active site (Fig. 2). As shown in Table 1, the substitution of methoxy group at the third position (compound **2**) with hydrogen (compound **3**) results in over 3-fold decrease in activity (IC_{50} equal to 6 and 20 μM, correspondingly). It can be explained by additional hydrophobic interactions of methoxy group with active site of enzyme.

The compounds **5** and **6** belong to other chemical class—derivatives of 3-[5-(2-methyl-3-phenyl-allidene)-4-oxo-2-thioxo-thizolidin-3-yl]-*N*-phenyl-propionamide. These inhibitors have different substituents on the phenyl ring: compound **5** has hydroxyl group at the second position, while compound **6** has carboxyl group at this place and hydroxyl group at the third position. Such structure change results in more than 2-fold decreasing of inhibitory activity (IC_{50} = 50 μM and 22.2 μM, respectively). Since compounds **5** and **6** possess low inhibitory activity toward *M. tuberculosis* LeuRS and

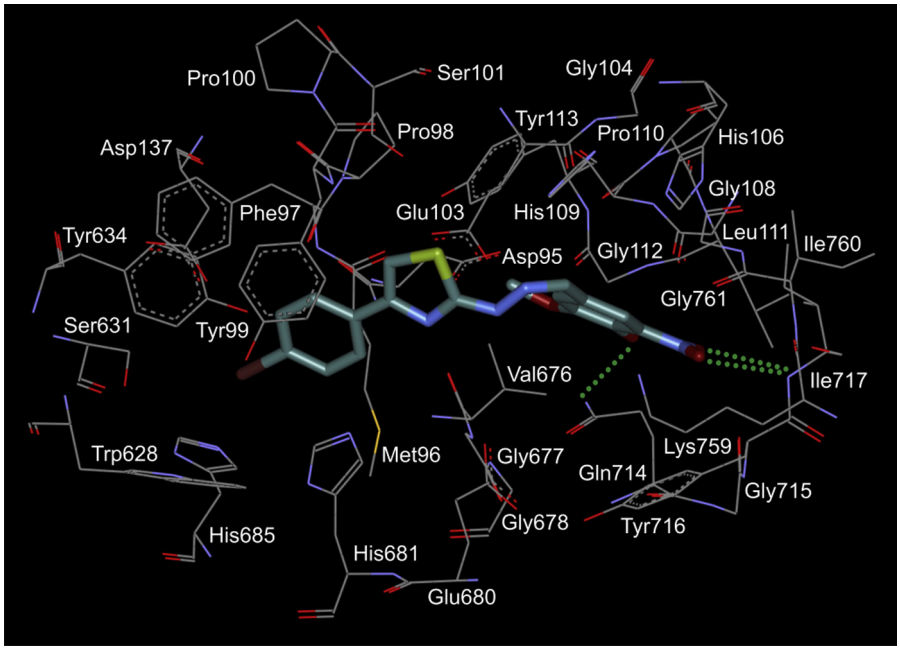

Figure 2. The binding mode of compound **1** in the active site of LeuRS *M. tuberculosis*. Hydrogen bonds are shown by the dotted lines.

belong to pan-assay interference (PAINS) compounds we did not consider them further.

In order to find more active inhibitors of *M. tuberculosis* LeuRS we have selected 26 derivatives of *N*-Benzylidene-*N*′-thiazol-2-yl-hydrazine from compound library containing about 100,000 compounds and tested in vitro. We have found five molecules able to inhibit *M. tuberculosis* LeuRS including compounds **7** (IC_{50} = 2.27 μM), **8** (IC_{50} = 19.3 μM), **9** (IC_{50} = 15.9 μM), **11** (IC_{50} = 15.9 μM) and **24** (IC_{50} = 11.4 μM) (Table 2).

The substitution of methoxy group and nitro group (compound **2**) with bromine atoms in R_3 phenyl ring (compound **7**) results in significant increasing of inhibitory activity (corresponding IC_{50} values are 6 μM and 2.27 μM). The substitution of nitro group in the structure of R_1 substituent and bromine atom in R_3 phenyl ring (compound **7**) accordingly with chlorine atom and methoxy group (compound **9**) results in two-fold decreasing of inhibitory activity (IC_{50} = 2.27 μM and 4.54 μM, respectively). The presence of nitro group in *meta*-position of R_1 substituent (compound **11**) instead of chlorine atom in *para*-position (compound **9**) and replacement of bromine atom to hydrogen atom in R_3 phenyl ring causes decreasing of inhibitory activity toward *M. tuberculosis* LeuRS in more than three times. It can be explained by the fact that bromine atoms take part in strong hydrophobic interactions with adenine-binding region of LeuRS active site (Fig. 3). Also, it should be noted that the presence of hydroxy group in *para*-position of R_3 ring compound **7** is very important for inhibitory activity, because the compound **8** with hydroxy group in *ortho*-position of R_3 substituent has significantly less inhibitory efficiency toward *M. tuberculosis* LeuRS.

The most active compounds **1**, **2**, **7**, **9**, and **24** were tested against human LeuRS (Table 3). The inhibitory activity of compounds toward pathogenic LeuRS is significantly better, than for eukaryotic enzyme. Therefore, the inhibitors from this chemical class seem to be selective toward *M. tuberculosis* LeuRS.

Table 2
Structures and in vitro inhibitory activity for *N*-Benzylidene-*N*′-thiazol-2-yl-hydrazine derivatives toward *M. tuberculosis* LeuRS

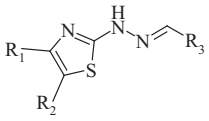

	R_1	R_2	R_3	IC_{50} (μM)
7	$4NO_2Ph$	H	3,5dBr-4OH-Ph	2.27
8	$4NO_2Ph$	H	3,5dBr-2OH-Ph	19.3
9	4ClPh	H	3Br-4OH-5MeO-Ph	4.54
10	4BrPh	H	3,4,5-tMeO-Ph	>20
11	$3NO_2Ph$	H	3MeO-4OH-Ph	15.9
12	$3NO_2Ph$	H	4OH-3,5dMeO-Ph	>20
13	$3NO_2Ph$	H	3OH-Ph	>20
14	$3NO_2Ph$	H	2OH-Ph	>20
15	$3NO_2Ph$	H	3Br-4OH-5MeO-Ph	>20
16	2,4dClPh	H	3MeO-4OH-Ph	>20
17	Ph	Ph	4MeO-3OH-Ph	>20
18	Ph	Ph	4OH-3,5dMeO-Ph	>20
19	Ph	H	4OH-3,5dMeO-Ph	>20
20	Ph	Ph	4OH-Ph	>20
21	Ph	H	3Br-4OH-5MeO-Ph	>20
22	CH_2CO_2Et	H	3,5dBr-4OH-Ph	>20
23	CH_3	$COCH_3$	2OH-5Br-Ph	>20
24	CH_3	CO_2Et	3MeO-4OH-Ph	11.4
25	CH_3	H	3Br-4OH-5MeO-Ph	>20
26	CH_3	$COCH_3$	3Br-4OH-5MeO-Ph	>20
27	CH_3	CH_3	4OH-Ph	>20
28	H	H	4OH-3,5dMeO-Ph	>20
29	H	H	3Br-4OH-5MeO-Ph	>20
30	H	H	3MeO-4OH-Ph	>20
31	H	H	2OH-5Br-Ph	>20
32	H	H	$4CO_2H$-Ph	>20

The antimicrobial effect of compounds **1**, **2**, **3**, **4**, **7**, **8**, **9**, **11** and **24** against *Mycobacterium tuberculosis* H37Rv grown under aerobic conditions was assessed by determining the minimum inhibitory concentration (MIC) and the concentrations which resulted in 50% and 90% inhibition of growth (IC_{50} and IC_{90}, respectively). The assay is based on measurement of growth in liquid medium of a fluorescent reporter strain of H37Rv where the readout is either optical density (OD) or fluorescence.[29–31] The use of two readouts minimizes problems caused by compound precipitation or autofluoresence. A linear relationship between OD and fluorescence readout has been established justifying the use of fluorescence as a measure of bacterial growth. MIC, IC_{50} and IC_{90} values generated from the OD are presented in Table 4.

The most active compound **1**, which seems to have the best cell permeability, was selected for intracellular (macrophage) drug screening assay, which evaluates intracellular drug effectiveness. This is important because *M. tuberculosis* can survive inside macrophages which contributes to treatment failure and disease relapse.

Intracellular drug activity for compound **1** is reported as log reduction values calculated as reduction in *M. tuberculosis* concentration from zero hour to 7 days post-infection. The three concentrations chosen (80 μg/mL, 8.0 μg/mL and 0.8 μg/mL) were based on the MIC data generated in the HTS primary screen. The mid concentration bracketed the reported MIC with the lower concentration 10-fold below the mid and the higher concentration 10-fold above the mid. Drug cytotoxicity is reported as cell proliferation, or percentage of viability. These data are presented in Table 5.

3. Conclusions

Using rational design approach of enzyme inhibitors we have found small-molecule compounds able to inhibit *M. tuberculosis* LeuRS among the derivatives of *N*-Benzylidene-*N*′-thiazol-2-yl-hydrazine. All active compounds were tested for antimicrobial effect against *M. tuberculosis* H37Rv. The compound 4-{[4-(4-Bromo-phenyl)-thiazol-2-yl]hydrazonomethyl}-2-methoxy-6-nitro-phenol seems to have the best cell permeability and inhibits growth of pathogenic bacteria with IC_{50} = 10.01 μM and IC_{90} = 13.53 μM.

4. Experimental

4.1. Synthetic chemistry

Starting materials and solvents were purchased from commercial suppliers and used without further purification. ^{1}H NMR spectra were recorded on a Varian VXR 400 instrument at 400 MHz. Chemical shifts are described as parts per million (δ) downfield from an internal standard of tetramethylsilane, and spin multiplicities are given as s (singlet), d (doublet), dd (double doublet), t (triplet), q (quartet), quintet (quintet), sext (sextet), sep (septet) or m (multiplet). HPLC–MS analysis was performed using the Agilent 1100 LC/MSD SL separations module and Mass Quad G1956B mass detector with electrospray ionization (+ve or −ve ion mode as indicated), and HPLC was performed using a Zorbax SB-C18, Rapid Resolution HT cartridge, 4.6 mm × 30 mm, 1.8 μm i.d. column (Agilent P/N 823975-902) at a temperature of 40 °C with gradient elution of 0–100% CH_3CN (with 1 mL/L HCOOH)/H_2O (with 1 mL/L HCOOH) at a flow rate of 3 mL/min and a run time of 2.8 min. Compounds were detected at 215 nm using a diode array G1315B detector. All tested compounds gave ⩾95% purity as determined by these methods.

N-Benzylidene-*N*′-thiazol-2-yl-hydrazine derivatives were synthesized in one pot manner (Scheme 1). Primarily 1,3-thiazole-2-hydrazine salt formed in reaction of correspondent α-chloro- or bromoketone with thiosemicarbazide in ^{i}PrOH solution.[32,33]

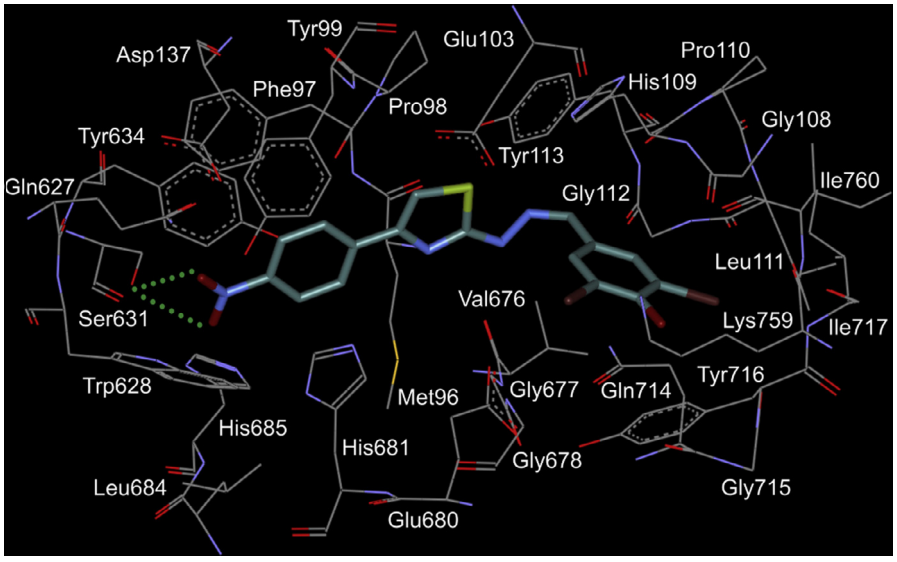

Figure 3. The binding mode of compound **7** in the active site of LeuRS *M. tuberculosis*. Hydrogen bonds are shown by the dotted lines.

Table 3
Inhibitory activities for the five selected compounds with human cytoplasmic LeuRS (*Hs*LeuRS) and *M. tuberculosis* LeuRS (*Mt*LeuRS)

Compound	IC_{50} (μM)	
	*Hs*LeuRS	*Mt*LeuRS
1	115.7	6.00
2	45.8	8.20
7	18.7	2.27
9	27.6	4.54
24	116.3	11.50

Hydrazine salt without isolation was basified with sodium carbonate, and then correspondent aldehyde was added. Unsubstituted 2-hydrazinothiazole hydrochloride was prepared separately starting from 2-aminothiazole.[34]

4.1.1. General procedure of *N*-Benzylidene-*N'*-thiazol-2-yl-hydrazine derivatives synthesis

12 mmol of correspondent halogenoketone and 0.91 g (10 mmol) of thiosemicarbazide were mixed in 30 ml of ^{i}PrOH and refluxed for 20 min. until bulky precipitate of 2-hydrazinothiazole salt formed. Then 2.12 g (20 mmol) of sodium carbonate were added. Reaction mixture was refluxed for additional 1–2 min, 10 mmol of correspondent aldehyde were added and refluxing was continued for 1–2 h. During that time heavy bulky precipitate substantially decreased in volume. After evaporation of solvent 20 ml of acetonitrile were added, mixture was heated to reflux and resulted solution or suspension was decanted from heavy inorganic solid material. Mixture was allowed to cool to room temperature, and then precipitate of product was filtered and dried on the air. Following substances were obtained:

Table 4
Compounds antimicrobial activity against *Mycobacterium tuberculosis* H37Rv (μM)

Compound	MIC	IC_{50}	IC_{90}
1	25	10.01	13.53
2	50	20.594	28.847
3	NA	>100	>100
4	NA	59.36	>100
7	>200	130	>200
8	>200	86	>200
9	>200	200	>200
11	>200	>200	>200
24	81	59	>200

4.1.1.1. 4-{[4-(4-Bromo-phenyl)-thiazol-2-yl]-hydrazonomethyl}-2-methoxy-6-nitro-phenol (1). Yield 3.45 g (77%) as wine powder mp 217–218 °C. LC–MS *m/z* 449 [M+H$^+$], t_R = 1.128 min. ^{1}H NMR (DMSO-d_6) δ: 12.00 (br s, 1H), 10.00 (br s, 1H), 8.01 (s, 1H), 7.80 (d, *J* = 8.4 Hz, 2H), 7.71 (s, 1H), 7.61 (d, *J* = 8.6 Hz, 2H), 7.51 (d, *J* = 1.8 Hz, 1H), 7.39 (s, 1H), 3.94 (s, 3H).

4.1.1.2. 2-Methoxy-6-nitro-4-{[4-(4-nitro-phenyl)-thiazol-2-yl]-hydrazonomethyl}-phenol (2). Yield 3.35 g (81%) as wine powder mp 231–232 °C. LC–MS *m/z* 416 [M+H$^+$], t_R = 1.055 min. ^{1}H NMR (DMSO-d_6) δ: 12.00 (br s, 1H), 10.00 (br s, 1H), 8.26 (d, *J* = 9.0 Hz, 2H), 8.13 (d, *J* = 9.0 Hz, 2H), 7.93 (s, 1H), 7.70 (br s, 1H), 7.63 (br s, 1H), 7.16 (s, 1H), 3.82 (s, 3H).

4.1.1.3. 2-Nitro-4-{[4-(4-nitro-phenyl)-thiazol-2-yl]-hydrazonomethyl}-phenol (3). Yield 1.79 g (46%) as orange brown powder mp 277–278 °C. LC–MS *m/z* 386 [M+H$^+$], t_R = 1.077 min. ^{1}H NMR (DMSO-d_6) δ: 12.25 (br s, 1H), 10.00 (br s, 1H), 8.26 (d, *J* = 8.6 Hz, 2H), 8.12 (d, *J* = 8.6 Hz, 2H), 8.02 (d, *J* = 1.2 Hz, 1H), 7.80 (dd, *J* = 8.0 Hz, 1.2 Hz, 1H), 7.70 (s, 1H), 7.11 (d, *J* = 8.2 Hz, 1H).

4.1.1.4. 2-Nitro-4-(thiazol-2-yl-hydrazonomethyl)-phenol (4). Compound (**4**) was synthesized starting from 2-hydrazinothiazole hydrochloride that was prepared separately from 2-aminothiazole.[31] Yield 0.79 g (30%) as brown powder mp 246–247 °C. LC–MS *m/z* 265 [M+H$^+$], t_R = 0.811 min. ^{1}H NMR (DMSO-d_6) δ: 11.00 (br s, 2H), 7.99 (d, *J* = 1.4 Hz, 1H), 7.92 (s, 1H), 7.68 (dd, *J* = 7.8 Hz, 1.4 Hz, 1H), 7.19 (d, *J* = 6.5 Hz, 1H), 6.96 (d, *J* = 8.0 Hz, 1H), 6.81 (d, *J* = 6.5 Hz, 1H).

4.1.1.5. *N*-(4-Hydroxy-phenyl)-3-[5-(2-methyl-3-phenyl-allylidene)-4-oxo-2-thioxo-thiazolidin-3-yl]-propionamide (5). Compound (**5**) was synthesized in a similar manner with Maga et al.[35] as orange powder mp 216–217 °C. LC–MS *m/z* 425 [M+H$^+$], t_R = 1.061 min. ^{1}H NMR (DMSO-d_6) δ: 9.80 (br s, 1H), 9.20 (s, 1H), 7.56 (d, *J* = 1.6 Hz, 1H), 7.47 (m, 6H), 7.30 (d, *J* = 8.8 Hz, 2H), 6.70 (d, *J* = 9.0 Hz, 2H), 4.30 (t, *J* = 6.7 Hz, 2H), 2.66 (t, *J* = 6.5 Hz, 2H), 2.21 (br. s., 3H).

Table 5
Macrophage and MTT results for compound **1**

Compd	Macrophage log reduction (low concn)	Macrophage log reduction (mid concn)	Macrophage log reduction (high concn)	MTT % viability (low concn)	MTT % viability (mid concn)	MTT % viability (high concn)
1	1.96	1.42	1.20	100	<10	10
Rifampin (pos control)	1.06	2.39	2.86	95	85	73

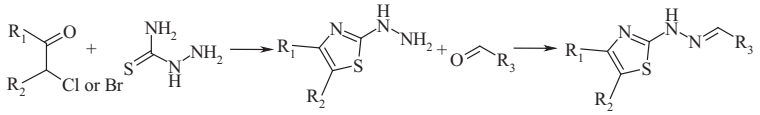

Scheme 1. Synthesis of *N*-Benzylidene-*N*′-thiazol-2-yl-hydrazine derivatives.

4.1.1.6. 2-Hydroxy-4-{3-[5-(2-methyl-3-phenyl-allylidene)-4-oxo-2-thioxo-thiazolidin-3-yl]-propionylamino}-benzoic acid (6). Compound (**6**) was synthesized analogously to (**5**) orange powder mp 257–258 °C. LC–MS *m*/*z* 469 [M+H$^+$], t_R = 0.942 min. ^{1}H NMR (DMSO-d_6) δ: 13.50 (br. s., 1H), 11.38 (br s, 1H), 10.32 (s, 1H), 7.70 (d, *J* = 7.8 Hz, 1H), 7.56 (s, 1H), 7.47 (m, 7H), 7.03 (d, *J* = 8.4 Hz, 1H), 4.33 (t, *J* = 7.0 Hz, 2H), 2.76 (t, *J* = 6.8 Hz, 2H), 2.21 (s, 3H).

4.1.1.7. 2,6-Dibromo-4-{[4-(4-nitro-phenyl)-thiazol-2-yl]-hydrazonomethyl}-phenol (7). Yield 1.59 g (32%) as light brown powder, mp 230–232 °C. LC–MS *m*/*z* 497 [M+H$^+$], t_R = 1.107 min. ^{1}H NMR (DMSO-d_6) δ: 12.65 (br s, 1H), 10.41 (br s, 1H), 8.26 (d, *J* = 6.5 Hz, 1H), 8.14 (d, *J* = 7.4 Hz, 2H), 7.89 (d, *J* = 7.4 Hz, 2H), 7.78 (m, 3H).

4.1.1.8. 2,4-Dibromo-6-{[4-(4-nitro-phenyl)-thiazol-2-yl]-hydrazonomethyl}-phenol (8). Yield 0.032 g (7%) as mustard powder, mp 247–249 °C. LC–MS *m*/*z* 497 [M+H$^+$], t_R = 1.112 min. ^{1}H NMR (DMSO-d_6) δ: 12.63 (br s, 1H), 10.75 (br s, 1H), 8.27 (m, 3H), 8.13 (d, *J* = 7.6 Hz, 2H), 7.77 (m, 3H).

4.1.1.9. 2-Bromo-4-{[4-(4-chloro-phenyl)-thiazol-2-yl]-hydrazonomethyl}-6-methoxy-phenol (9). Yield 0.70 g (17%) as cocoa powder, mp 253–255 °C. LC–MS *m*/*z* 438 [M+H$^+$], t_R = 0.994 min. ^{1}H NMR (DMSO-d_6) δ: 12.37 (br s, 1H), 9.93 (br s, 1H), 7.90 (s, 1H), 7.76 (d, *J* = 7.6 Hz, 2H), 7.40 (d, *J* = 7.6 Hz, 2H), 7.36 (s, 2H), 7.21 (s, 1H), 3.86 (s, 3H).

4.1.1.10. *N*-[4-(4-Bromo-phenyl)-thiazol-2-yl]-*N*′-(3,4,5-trimethoxy-benzylidene)-hydrazine (10). Yield 3.14 g (70%) as creamy powder, mp 170–171 °C. LC–MS *m*/*z* 448 [M+H$^+$], t_R = 1.104 min. ^{1}H NMR (DMSO-d_6) δ: 12.15 (br s, 1H), 7.97 (s, 1H), 7.78 (d, *J* = 7.8 Hz, 2H), 7.62 (d, *J* = 7.8 Hz, 2H), 7.38 (s, 1H), 6.96 (s, 2H), 3.84 (s, 6H), 3.70 (s, 3H).

4.1.1.11. 2-Methoxy-4-{[4-(3-nitro-phenyl)-thiazol-2-yl]-hydrazonomethyl}-phenol (11). Yield 2.09 g (57%) as brown powder, mp 200–202 °C. LC–MS *m*/*z* 371 [M+H$^+$], t_R = 0.99 min. ^{1}H NMR (DMSO-d_6) δ: 12.10 (br s, 1H), 9.65 (br s, 1H), 8.68 (s, 1H), 8.29 (d, *J* = 10.0 Hz, 1H), 8.14 (dd, *J* = 10.4 Hz, 1.8 Hz, 1H), 7.95 (s, 1H), 7.71 (t, *J* = 10.0 Hz, 1H), 7.63 (s, 1H), 7.25 (d, *J* = 1.5 Hz, 1H), 7.08 (dd, *J* = 10.0 Hz, 1.5 Hz, 1H), 6.84 (d, *J* = 10.0 Hz, 1H), 3.84 (s, 3H).

4.1.1.12. 2,6-Dimethoxy-4-{[4-(3-nitro-phenyl)-thiazol-2-yl]-hydrazonomethyl}-phenol (12). Yield 1.54 g (39%) as brown powder, mp 155–157 °C. LC–MS *m*/*z* 401 [M+H$^+$], t_R = 1.079 min. ^{1}H NMR (DMSO-d_6) δ: 12.15 (br s, 1H), 8.81 (br s, 1H), 8.68 (d, *J* = 2.4 Hz, 1H), 8.29 (dd, *J* = 8.6 Hz, 1.8 Hz, 1H), 8.16 (dd, *J* = 8.2 Hz, 1.7 Hz, 1H), 7.95 (d, *J* = 1.4 Hz, 1H), 7.71 (t, *J* = 8.7 Hz, 1H), 7.63 (s, 1H), 6.96 (s, 2H), 3.83 (s, 6H).

4.1.1.13. 3-{[4-(3-Nitro-phenyl)-thiazol-2-yl]-hydrazonomethyl}-phenol (13). Yield 1.67 g (49%) as orange powder, mp 238–240 °C. LC–MS *m*/*z* 341 [M+H$^+$], t_R = 0.91 min. ^{1}H NMR (DMSO-d_6) δ: 10.50 (br s, 2H), 8.69 (d, *J* = 2.2 Hz, 1H), 8.31 (d, *J* = 8.8 Hz, 1H), 8.15 (dd, *J* = 8.6 Hz, 1.6 Hz, 1H), 7.97 (s, 1H), 7.69 (t, *J* = 8.8 Hz, 1H), 7.65 (s, 1H), 7.24 (t, *J* = 8.4 Hz, 1H), 7.14 (s, 1H), 7.09 (d, *J* = 7.8 Hz, 1H), 6.82 (d, *J* = 8.6 Hz, 1H).

4.1.1.14. 2-{[4-(3-Nitro-phenyl)-thiazol-2-yl]-hydrazonomethyl}-phenol (14). Yield 1.79 g (53%) as yellow powder, mp 231–233 °C. LC–MS *m*/*z* 341 [M+H$^+$], t_R = 1.089 min. ^{1}H NMR (DMSO-d_6) δ: 12.15 (br s, 1H), δ 10.0 (br s, 1H), 8.66 (d, *J* = 2.4 Hz, 1H), 8.34 (s, 1H), 8.29 (d, *J* = 9.0 Hz, 1H), 8.12 (dd, *J* = 8.8 Hz, 1.5 Hz, 1H), 7.70 (t, *J* = 9.0 Hz, 1H), 7.62 (t, *J* = 8.6 Hz, 1H), 7.22 (t, *J* = 8.4 Hz, 1H), 6.90 (m, 2H).

4.1.1.15. 2-Bromo-6-methoxy-4-{[4-(3-nitro-phenyl)-thiazol-2-yl]-hydrazonomethyl}-phenol (15). Yield 2.37 g (53%) as light brown powder, mp 121–122 °C. LC–MS *m*/*z* 449 [M+H$^+$], t_R = 1.114 min. ^{1}H NMR (DMSO-d_6) δ: 12.24 (br s, 1H), 9.90 (br s, 1H), 8.68 (d, *J* = 2.0 Hz, 1H), 8.33 (d, *J* = 8.5 Hz, 1H), 8.13 (dd, *J* = 8.4 Hz, 1.8 Hz, 1H), 7.94 (s, 1H), 7.73 (d, *J* = 9.2 Hz, 1H), 7.64 (t, *J* = 8.4 Hz, 1H), 7.41 (d, *J* = 2.6 Hz, 1H), 7.27 (d, *J* = 2.8 Hz, 1H), 3.90 (s, 3H).

4.1.1.16. 4-{[4-(2,4-Dichloro-phenyl)-thiazol-2-yl]-hydrazonomethyl}-2-methoxy-phenol (16). Yield 0.6 g (15%) as light brown powder, mp 127–128 °C. LC–MS *m*/*z* 394 [M+H$^+$], t_R = 1.054 min. ^{1}H NMR (DMSO-d_6) δ: 11.80 (br s, 1H), 9.90 (br s, 1H), 7.92 (d, *J* = 8.7 Hz, 1H), 7.89 (s, 1H), 7.45 (d, *J* = 2.0 Hz, 1H), 7.36 (dd, *J* = 8.5 Hz, 1.8 Hz, 1H), 7.20 (m, 2H), 6.99 (d, *J* = 9.2 Hz, 1H), 6.78 (d, *J* = 9.0 Hz, 1H), 3.88 (s, 3H).

4.1.1.17. 5-[(4,5-Diphenyl-thiazol-2-yl)-hydrazonomethyl]-2-methoxy-phenol (17). Yield 1.83 g (46%) as sandy powder, mp 165–167 °C. LC–MS *m*/*z* 402 [M+H$^+$], t_R = 1.011 min. ^{1}H NMR (DMSO-d_6) δ: 11.98 (br s, 1H), 9.21 (br s, 1H), 7.91 (s, 1H), 7.31 (m, 10H), 7.21 (s, 1H), 6.96 (q, *J* = 7.6 Hz, 2H), 3.80 (s, 3H).

4.1.1.18. 4-[(4,5-Diphenyl-thiazol-2-yl)-hydrazonomethyl]-2,6-dimethoxy-phenol (18). Yield 2.63 g (61%) as beige powder, mp 222–223 °C. LC–MS *m*/*z* 432 [M+H$^+$], t_R = 1.074 min. ^{1}H NMR (DMSO-d_6) δ: 10.0 (br s, 2H), 7.93 (s, 1H), 7.43 (m, 2H), 7.32 (m, 8H), 6.94 (s, 2H), 3.81 (s. 6H).

4.1.1.19. 2,6-Dimethoxy-4-[(4-phenyl-thiazol-2-yl)-hydrazonomethyl]-phenol (19). Yield 0.87 g (25%) as sandy powder, mp 212–213 °C. LC–MS *m*/*z* 356 [M+H$^+$], t_R = 0.954 min. ^{1}H NMR (DMSO-d_6) δ: 10.00 (br s, 2H), 7.94 (s, 1H), 7.85 (d, *J* = 7.8 Hz, 2H), 7.41 (t, *J* = 7.7 Hz, 2H), 7.29 (m, 2H), 6.95 (s, 2H), 3.82 (s. 6H).

4.1.1.20. 4-[(4,5-Diphenyl-thiazol-2-yl)-hydrazonomethyl]-phenol (20). Yield 2.71 g (73%) as beige powder, mp 126–127 °C. LC–MS *m/z* 372 [M+H$^+$], t_R = 1.064 min. ^{1}H NMR (DMSO-d_6) δ: 11.96 (br s, 1H), 9.86 (br s, 1H), 7.96 (s, 1H), 7.49 (m, 4H), 7.31 (m, 8H), 6.85 (d, *J* = 8.4 Hz, 2H).

4.1.1.21. 2-Bromo-6-methoxy-4-[(4-phenyl-thiazol-2-yl)-hydrazonomethyl]-phenol (21). Yield 0.49 g (12%) as brown prisms, mp 196–197 °C. LC–MS *m/z* 404 [M+H$^+$], t_R = 0.973 min. ^{1}H NMR (DMSO-d_6) δ: 12.05 (br s, 1H), 9.99 (br s, 1H), 7.94 (s, 1H), 7.85 (d, *J* = 7.6 Hz, 2H), 7.41 (m, 3H), 7.30 (m, 3H), 3.89 (s, 3H).

4.1.1.22. {2-[*N'*-(3,5-Dibromo-4-hydroxy-benzylidene)-hydrazino]-thiazol-4-yl}-acetic acid ethyl ester (22). Yield 4.10 g (89%) as ivory powder, mp 187–188 °C. LC–MS *m/z* 462 [M+H$^+$], t_R = 0.847 min. ^{1}H NMR (DMSO-d_6) δ: 11.00 (br s, 2H), 7.84 (s, 1H), 7.80 (s, 2H), 6.64 (s, 1H), 4.07 (q, *J* = 7.7 Hz, 2H), 3.58 (s, 2H), 1.19 (t, *J* = 7.5 Hz, 3H).

4.1.1.23. 1-{2-[*N'*-(5-Bromo-2-hydroxy-benzylidene)-hydrazino]-4-methyl-thiazol-5-yl}-ethanone (23). Yield 2.89 g (82%) as golden prisms, mp 262–263 °C. LC–MS *m/z* 354 [M+H$^+$], t_R = 0.779 min. ^{1}H NMR (DMSO-d_6) δ: 12.53 (br s, 1H), 10.59 (br s, 1H), 8.36 (s, 1H), 7.76 (d, *J* = 1.4 Hz, 1H), 7.38 (dd, *J* = 8.2 Hz, 1.4 Hz, 1H), 6.91 (d, *J* = 8.4 Hz, 1H), 2.50 (s, 3H), 2.42 (s, 3H).

4.1.1.24. 2-[*N'*-(4-Hydroxy-3-methoxy-benzylidene)-hydrazino]-4-methyl-thiazole-5-carboxylic acid ethyl ester (24). Yield 1.05 g (32%) as ivory powder, mp 178–179 °C. LC–MS *m/z* 336 [M+H$^+$], t_R = 0.727 min. ^{1}H NMR (DMSO-d_6) δ: 12.30 (br s, 1H), 9.52 (br s, 1H), 7.98 (s, 1H), 7.25 (d, *J* = 1.2 Hz, 1H), 7.10 (d, *J* = 9.3 Hz, 1H), 6.84 (dd, *J* = 9.4 Hz, 1.0 Hz, 1H), 4.21 (q, *J* = 6.8 Hz, 2H), 3.84 (s, 3H), 2.46 (s, 3H), 1.27 (t, *J* = 7.0 Hz, 3H).

4.1.1.25. 2-Bromo-6-methoxy-4-[(4-methyl-thiazol-2-yl)-hydrazonomethyl]-phenol (25). Yield 0.37 g (11%) as gray powder, mp 176–178 °C. LC–MS *m/z* 342 [M+H$^+$], t_R = 0.672 min. ^{1}H NMR (DMSO-d_6) δ: 10.00 (br s, 2H), 7.99 (s, 1H), 7.44 (s, 1H), 7.29 (s, 1H), 6.46 (s, 1H), 3.90 (s, 3H), 2.21 (s, 1H).

4.1.1.26. 1-{2-[*N'*-(3-Bromo-4-hydroxy-5-methoxy-benzylidene)-hydrazino]-4-methyl-thiazol-5-yl}-ethanone (26). Yield 2.34 g (61%) as mustard powder, mp 215–216 °C. LC–MS *m/z* 384 [M+H$^+$], t_R = 0.731 min. ^{1}H NMR (DMSO-d_6) δ: 7.97 (s, 1H), 7.38 (s, 1H), 7.23 (s, 1H), 5.00 (br s, 2H), 3.86 (s, 3H), 2.48 (s, 3H), 2.39 (s, 3H).

4.1.1.27. 4-[(4,5-Dimethyl-thiazol-2-yl)-hydrazonomethyl]-phenol (27). Yield 1.45 g (59%) as beige powder, mp 145–147 °C. LC–MS *m/z* 248 [M+H$^+$], t_R = 0.608 min. ^{1}H NMR (DMSO-d_6) δ: 11.00 (br s, 1H), 9.77 (s, 1H), 7.88 (s, 1H), 7.43 (d, *J* = 9.0 Hz, 2H), 6.81 (d, *J* = 9.0 Hz, 2H), 2.15 (s, 3H), 2.05 (s, 3H).

4.1.1.28. 2,6-Dimethoxy-4-(thiazol-2-yl-hydrazonomethyl)-phenol (28). Yield 2.17 g (78%) as cocoa powder, mp 207–208 °C. LC–MS *m/z* 280 [M+H$^+$], t_R = 0.763 min. ^{1}H NMR (DMSO-d_6) δ: 10.00 (br s, 2H), 7.91 (s, 1H), 7.20 (d, *J* = 6.5 Hz, 1H), 6.92 (s, 2H), 6.80 (d, *J* = 6.3 Hz, 1H), 3.81 (s, 6H).

4.1.1.29. 2-Bromo-6-methoxy-4-(thiazol-2-yl-hydrazonomethyl)-phenol (29). Yield 1.40 g (43%) as sandy powder, mp 202–203 °C. LC–MS *m/z* 328 [M+H$^+$], t_R = 0.796 min. ^{1}H NMR (DMSO-d_6) δ: 10.00 (br s, 2H), 7.89 (s, 1H), 7.36 (s, 1H), 7.22 (m, 2H), 6.83 (d, *J* = 6.0 Hz, 1H), 3.87 (s, 6H).

4.1.1.30. 2-Methoxy-4-(thiazol-2-yl-hydrazonomethyl)-phenol (30). Yield 0.75 g (30%) as black prisms, mp 158–160 °C. LC–MS *m/z* 250 [M+H$^+$], t_R = 0.644 min. ^{1}H NMR (DMSO-d_6) δ: 10.00 (br s, 2H), 7.92 (s, 1H), 7.22 (s, 2H), 7.03 (d, *J* = 6.8 Hz, 1H), 6.81 (m, 2H), 3.82 (s, 3H).

4.1.1.31. 4-Bromo-2-(thiazol-2-yl-hydrazonomethyl)-phenol (31). Yield 0.65 g (22%) as dark gray powder, mp 236–237 °C. LC–MS *m/z* 298 [M+H$^+$], t_R = 0.683 min. ^{1}H NMR (DMSO-d_6) δ: 12.00 (br s, 1H), 10.50 (s, 1H), 8.25 (s, 1H), 7.72 (d, *J* = 1.2 Hz, 1H), 7.33 (d, *J* = 7.0 Hz, 1H), 7.21 (s, 1H), 6.88 (m, 2H).

4.1.1.32. 4-(Thiazol-2-yl-hydrazonomethyl)-benzoic acid (32). Yield 1.09 g (43%) as mustard powder, mp 277–278 °C (subl.). LC–MS *m/z* 248 [M+H$^+$], t_R = 0.706 min. ^{1}H NMR (DMSO-d_6) δ: 11.30 (br s, 3H), 8.44 (s, 1H), 8.02 (d, *J* = 8.7 Hz, 2H), 7.92 (d, *J* = 8.6 Hz, 2H), 7.49 (d, *J* = 6.0 Hz, 1H), 7.17 (d, *J* = 6.0 Hz, 1H).

4.2. Receptor preparation for flexible docking

Homology model of *Mycobacterium tuberculosis* LeuRS has been built using SWISS-MODEL workspace.[36] As a template for homology modeling was used crystal structure of *Thermus thermophilus* LeuRS (PDB ID: 2V0C).[18]

A receptor molecule has been minimized in water with GROMACS molecular dynamics simulation package (GROMACS force field, steepest descent algorithm, 1000 steps, em_tolerance = 100, em_step = 0,001). The partial atom charges of the receptor molecule were taken from the Amber force field. Active site spheres were calculated with DOCK *sphgen* software. The spheres with the positions outside of the active site of LeuRS were deleted manually. Connolly MS and Grid programs from DOCK package were used to generate receptor Connolly surface and energy grids. Surface and grid calculations were performed with parameter settings detailed in the reference.[37] The grid spacing was set to 0.3.

4.3. Ligand database processing

Calculations of ligand geometry were performed using YFF force field described in the reference.[38] Partial atomic charges of the ligands were calculated with Kirchhoff method.[39]

4.4. Flexible docking

DOCK program has been used for receptor-ligand flexible docking. DOCK input parameters have been set as described previously.[37] In our virtual screening experiments 'multiple anchors' parameter was set as following: the minimum of heavy atoms in the anchor was set to 6, the maximum number of orientations was set to 1000, and the ≪all atoms≫ model has been chosen. 270 compounds with scores less than −40 kcal/mol have been taken for the in vitro analysis of their inhibitory activity.

The structures were visualized using the Discovery Studio Visualizer 4.0.[40]

4.5. Purification of *Mycobacterium tuberculosis* LeuRS

The plasmid pET28a encoding the gene for *M. tuberculosis* LeuRS (the plasmid was the kind gift of Stephen Cusack and Andres Palencia) was used to express the protein in *Escherichia coli* strain Rosetta (DE3). A single colony was used to inoculate LB medium containing 50 mg/L kanamycin and 36 mg/L chloramphenicol, which was then incubated overnight at 37 °C. A culture was induced to a final concentration of 1 mM IPTG and was incubated for 7 h at 23 °C. The cells were harvested by centrifugation.

The cells pellet was resuspended in 20–25 mL of buffer containing 20 mM Tris–HCl (pH 8.0), 100 mM NaCl, 5 mM $MgCl_2$, 1 mM β-mercaptoethanol and 1 tablet of Complete EDTA-free protease

cocktail inhibitors and was sonicated for 10 min (in total) with 30 s of active cycle and 60 s of cool down. The lysate was cleared by centrifugation for 30 min at 16,000 rpm. The imidazole was added to supernatant to reach 15 mM in final and was mixed with 5 mL of Ni-NTA in binding buffer A (20 mM Tris–HCl (pH 8.0), 300 mM NaCl, 5 mM $MgCl_2$, 15 mM imidazole, 1 mM β-mercaptoethanol, 0.1 mM PMSF). The mixture was stirred for 1 h at 4 °C and was applied into the empty column. The column was washed by 15 mL of buffer B (20 mM Tris–HCl (pH 8.0), 0.3 M NaCl, 5 mM $MgCl_2$, 15 mM imidazole, 1 mM β-mercaptoethanol, 0.1 mM PMSF). Elution of protein was carried by buffer E (20 mM Tris–HCl (pH 8.0), 0.3 M NaCl, 5 mM $MgCl_2$, 0.2 M imidazole, 5 mM β-mercaptoethanol, 0.1 mM PMSF). The homogeneity of the protein was tested by 12.5% SDS–PAGE. The fractions were pooled and dialyzed for 2 h with 20 mM Tris–HCl (pH 8.0), 100 mM NaCl, 5 mM $MgCl_2$, 5 mM mercaptoethanol and overnight with 20 mM Tris–HCl (pH 7.4), 100 mM NaCl, 5 mM $MgCl_2$, 5 mM mercaptoethanol. The purified protein was concentrated using a Centricon-30 (Amicon).

4.6. Purification of human cytoplasmic LeuRS

The plasmid pET16 encoding human cytoplasmic LeuRS, C-terminal histidine tag (the plasmid was the kind gift of Dr. Michael Alley), was transformed in *E. coli* strain Rosetta DE3. A single colony was inoculated into 10 ml of 2xYT medium contained 69 mg/L chloramphenicol, 100 mg/L ampicillin and incubated at 37 °C overnight. 10 ml overnight culture was transferred to 1 l of 2xYT medium and grown at 37 °C until OD_{600} = 0.6. A culture was then induced with 0.4 mM IPTG and further grown at 20 °C for 5 h. The cells were pelleted by centrifugation at 5000 rpm for 15 min at 4 °C. The cells pellet was lysed with 20 ml buffer A (20 mM Na-p (pH 7.9), containing 300 mM NaCl, 5 mM imidazole, 5% glycerol, 1 mM β-mercaptoethanol and 1 tablet of Complete EDTA-free protease cocktail inhibitors). The suspended cells were sonicated at 40% power 3 min using an ultrasonic processor XL-Sonicator and centrifuged at 14,000 rpm for 30 min at 4 °C. The supernatant was combined with 5 ml Ni-NTA agarose (pre-equilibrated with buffer A). The gel and lysate were mixed 1 h at 4 °C, and loaded on column. The column was then washed with 5 column volumes of buffer A and eluted with 250 mM imidazole in buffer A. The eluted fractions containing desired protein were pooled and dialyzed against buffer B (100 mM K-p (pH 6.8), 10 mM mercaptoethanol and 20% glycerol). Protein was concentrated using a Centricone-30 (Amicon).

4.7. Aminoacylation assay

The standard aminoacylation assays were performed in 100 mM Tris–HCl (pH 8.0), 10 mM $MgCl_2$, 2 mM DTT, 5 mM ATP, 10 mM KCl, 90 μM [^{14}C]-L-leucine (238 mCi/mmol), 4 mg/ml *E. coli* tRNA and 25 nM *M. tuberculosis* LeuRS. The reaction was incubated at 37 °C and aliquots were quenched by 10% trichloracetic acid, and the level of aminoacylation of tRNA was determined by scintillation counting.

For the inhibitory studies in aminoacylation reaction 20 μl solution containing 25 nM *M. tuberculosis* LeuRS, 100 mM Tris–HCl (pH 8.0), 10 mM $MgCl_2$, 90 μM [^{14}C]-L-leucine (238 mCi/mmol), 2 mM DTT, 4 mg/ml *E. coli* tRNA and appropriate concentrations of inhibitor (dissolved in DMSO) were incubated for 5 min at 37 °C. Reactions were initiated by addition of ATP to final concentration of 2 mM. At least triplicates were averaged to generate an IC_{50} value using Origin 7.0.

4.8. Minimal inhibitory concentration (MIC)

The MIC of compound was determined by measuring bacterial growth after 5 d in the presence of test compounds. Compounds were prepared as 10-point two-fold serial dilutions in DMSO and diluted into 7H9-Tw-OADC medium in 96-well plates with a final DMSO concentration of 2%. The highest concentration of compound was 200 μM where compounds were soluble in DMSO at 10 mM. For compounds with limited solubility, the highest concentration was 50× less than the stock concentration, for example, 100 μM for 5 mM DMSO stock, 20 μM for 1 mM DMSO stock. For potent compounds, assays were repeated at lower starting concentrations. Each plate included assay controls for background (medium/DMSO only, no bacterial cells), zero growth (100 μM rifampicin) and maximum growth (DMSO only), as well as a rifampicin dose response curve. Plates were inoculated with *M. tuberculosis* and incubated for 5 days: growth was measured by OD_{590} and fluorescence (Ex 560/Em 590) using a BioTek™ Synergy 4 plate reader. Growth was calculated separately for OD_{590} and RFU. To calculate the MIC, the 10-point dose response curve was plotted as % growth and fitted to the Gompertz model using GraphPad Prism 5. The MIC was defined as the minimum concentration at which growth was completely inhibited and was calculated from the inflection point of the fitted curve to the lower asymptote (zero growth). In addition dose response curves were generated using the Levenberg–Marquardt algorithm and the concentrations that resulted in 50% and 90% inhibition of growth were determined (IC_{50} and IC_{90} respectively).

4.9. Intracellular drug activity

The murine J774 cell line was propagated in RPMI 1640 supplemented with L-glutamine and fetal bovine serum (FBS). Cells were maintained in tissue culture flasks at 37 °C in the presence of 5% CO_2. For infection studies, J774 cells were transferred to 12-well tissue culture chambers in 1 mL volumes at a density of $2.0 * 10^5$ in the presence of 10% FBS. After overnight incubation, the medium was replaced with fresh medium containing 1% FBS to stop macrophage division while maintaining cell viability. Twenty-four hours later, the macrophage monolayer was enumerated with an ocular micrometer for total number of cells per well to determine the infection ratio. The medium was removed and replaced with 1 mL of fresh medium with 1% FBS containing *M. tuberculosis* at a multiplicity of infection (MOI) of 5 Mycobacteria/macrophage. The cells are infected for 4 h after which time nonphagocytosed *Mycobacteria* were washed from the monolayers and fresh medium added. Drugs were then added, using 3 concentrations, and infection allowed to proceed for 7 days. At 0 and 7 days, the macrophages were lysed with sodium dodecyl sulfate, treated with DNAase, diluted and plated onto 7H10 agar to determine the cell number or colony forming units (CFU). Each drug concentration was tested in duplicate and rifampin was used as the positive control drug. A drug cytotoxicity control plate assay (MTT proliferation) was also conducted in parallel using uninfected macrophages to confirm that concentrations utilized for testing were not toxic to the macrophages.

Acknowledgements

We thank Dr. Stephen Cusack and Dr. Andres Palencia (EMBL Grenoble Outstation, France) for the gift of clone for expression and purification of *M. tuberculosis* LeuRS.

We thank Dr. Michael Alley (Anacor Pharmaceuticals, USA) for the gift of plasmid for expression and purification of human cytoplasmic LeuRS.

This work was supported by the Science and Technology Center in Ukraine (contract No. 5218), the National Agency of Science, Innovation and Informatization of Ministry of Education and Science of Ukraine (contract No. DP/337-2013) and by National Institutes of Health and the National Institute of Allergy and Infectious Diseases (contract No. HHSN272201100009I).

References and notes

1. Hurdle, J. G.; O'Neill, A. J.; Chopra, I. *Antimicrob. Agents Chemother.* **2005**, *49*, 124821.
2. Vondenhoff, G. H.; Van Aerschot, A. *Eur. J. Med. Chem.* **2011**, *46*, 5227.
3. Dewan, V.; Reader, J.; Forsyth, K. M. *Top. Curr. Chem.* **2014**, *344*, 293.
4. Datt, M.; Sharma, A. *BMC Genomics* **2014**, *15*, 1069.
5. Fang, Z. P.; Wang, M.; Ruan, Z. R.; Tan, M.; Liu, R. J.; Zhou, M.; Zhou, X. L.; Wang, E. D. *Nucleic Acid Res.* **2014**, *42*, 5109.
6. Pham, J. S.; Dawson, K. L.; Jackson, K. E.; Lim, E. E.; Pasaje, C. F. A.; Turner, K. E. C.; Ralph, S. A. *Int. J. Parasitol. Drugs Drug Resist.* **2014**, *4*, 1.
7. Konishi, M.; Nishio, M.; Saitoh, K.; Miyaki, T.; Oki, T.; Kawaguchi, H. *J. Antibiot.* **1989**, *42*, 1749.
8. Hasenoehrl, A.; Galic, T.; Ergovic, G.; Marsic, N.; Skerlev, M.; Mittendorf, J.; Geschke, U.; Schmidt, A.; Schoenfeld, W. *Antimicrob. Agents Chemother.* **2006**, *50*, 3011.
9. Kitabatake, M.; Ali, K.; Demain, A.; Sakamoto, K.; Yokoyama, S.; Soll, D. *J. Biol. Chem.* **2002**, *277*, 23882.
10. Keller, T. L.; Zocco, D.; Sundrud, M. S.; Hendrick, M.; Edenius, M.; Yum, J.; Kim, Y. J.; Lee, H. K.; Cortese, J. F.; Wirth, D. F.; Dignam, J. D.; Rao, A.; Yeo, C. Y.; Mazitschek, R.; Whitman, M. *Nat. Chem. Biol.* **2012**, *8*, 311.
11. Konrad, I.; Roschenthaler, R. *FEBS Lett.* **1977**, *83*, 341.
12. Sutherland, R.; Boon, R. J.; Griffin, K. E.; Masters, P. J.; Slocombe, B.; White, A. R. *Antimicrob. Agents Chemother.* **1985**, *27*, 495.
13. Hussain, T.; Yogavel, M.; Sharma, A. *Antimicrob. Agents Chemother.* **2015**, *29*, 1856.
14. Zhang, F.; Du, J.; Wang, Q.; Hu, Q.; Zhang, J.; Ding, D.; Zhao, Y.; Yang, F.; Wang, E.; Zhou, H. *Org. Biomol. Chem.* **2013**, *11*, 5310.
15. Zhao, Y.; Wang, Q.; Meng, Q.; Ding, D.; Yang, H.; Gao, G.; Li, D.; Zhu, W.; Zhou, H. *Bioorg. Med. Chem.* **2012**, *20*, 1240.
16. Xiao, Z. P.; Ouyang, H.; Wang, X. D.; Ly, P. C.; Huang, J.; Yu, S. R.; Yi, T. F.; Yang, Y. L.; Zhu, H. L. *Bioorg. Med. Chem.* **2011**, *19*, 3884.
17. Xiao, Z. P.; He, X. B.; Peng, Z. Y.; Xiong, T. J.; Peng, J.; Chen, L. H.; Zhu, H. L. *Bioorg. Med. Chem.* **2011**, *19*, 1571.
18. Rock, F. L.; Mao, W.; Yaremchuk, A.; Tukalo, M.; Crepin, T.; Zhou, H.; Zhang, Y. K.; Hernandez, V.; Akama, T.; Baker, S. J.; Plattner, J. J.; Shapiro, L.; Martinis, S. A.; Benkovic, S. J.; Cusack, S.; Alley, M. R. *Science* **2007**, *316*, 1759.
19. Reader, J. S.; Ordoukhanian, P. T.; Kim, J. G.; De Crecy-Lagard, V.; Hwang, I.; Farrand, S.; Schimmel, P. *Science* **2005**, *309*, 1533.
20. Hu, Q. H.; Liu, R. J.; Fang, Z. P.; Zhang, J.; Ding, Y. Y.; Tan, M.; Wang, M.; Pan, W.; Zhou, H. C.; Wang, E. D. *Sci. Rep.* **2013**, *3*, 2475.
21. Ding, D.; Meng, O.; Gao, G.; Zhao, Y.; Wang, Q.; Nare, B.; Jacobs, R.; Rock, F.; Alley, M. R.; Plattner, J. J.; Chen, G.; Li, D.; Zhou, H. *J. Med. Chem.* **2011**, *54*, 1276.
22. Stoichet, B. K.; Stroud, R. M.; Santi, D. V.; Kuntz, I. D.; Perry, K. M. *Science* **1993**, *259*, 1445.
23. Bodian, D. L.; Yamasaki, R. B.; Buswell, R. L.; Stearns, J. F.; White, J. M.; Kuntz, I. D. *Biochemistry* **1993**, *32*, 2967.
24. Ring, C. S.; Sun, E.; McKerrow, J. H.; Lee, G. K.; Rosenthal, P. J.; Kuntz, I. D.; Cohen, F. E. *Proc. Natl. Acad. Sci. U.S.A.* **1993**, *90*, 3583.
25. Ewing, T. J.; Makino, S.; Skillman, A. G.; Kuntz, I. D. *J. Comput. Aided Mol. Des.* **2001**, *15*, 411.
26. Cusack, S.; Yaremchuk, A.; Tukalo, M. *EMBO J.* **2000**, *19*, 2351.
27. Verma, A.; Saraf, S. K. *Eur. J. Med. Chem.* **2008**, *43*, 897.
28. Ioerger, T. R.; O'Malley, T.; Liao, R.; Guinn, K. M.; Hickey, M. J.; Mohaideen, N.; Murphy, K. C.; Boshoff, H. I. M.; Mizrahi, V.; Rubin, E. J.; Sassetti, C. M.; Barry, C. E., III; Sherman, D. R.; Parish, T.; Sacchettini, J. C. *PLoS One* **2013**, *8*, e75245.
29. Ollinger, J.; Bailey, M. A.; Moraski, G. C.; Casey, A.; Florio, S.; Alling, T.; Miller, M. J.; Parish, T. *PLoS One* **2013**, *8*, e60531.
30. Zelmer, A.; Carroll, P.; Andreu, N.; Hagens, K.; Mahlo, J.; Redinger, N.; Robertson, B. D.; Wiles, S.; Ward, T. H.; Parish, T.; Ripoll, J.; Bancroft, G. J.; Schaible, U. E. *J. Antimicrob. Chemother.* **2012**, *67*, 1948.
31. Lambert, R. J.; Pearson, J. *J. Appl. Microbiol.* **2000**, *88*, 788.
32. Bose, Nandi *J. Ind. Chem. Soc.* **1930**, *7*, 733.
33. Takrouri, K.; Chen, T.; Papadopoulos, E.; Sahoo, R.; Kabha, E.; Chen, H.; Cantel, S.; Wagner, G.; Halperin, J. A.; Aktas, B. H.; Chorev, M. *Eur. J. Med. Chem.* **2014**, *77*, 361.
34. Haviv, F.; Ratajczyk, J. D.; DeNet, R. W.; Kerdesky, F. A.; Walters, R. L.; Schmidt, S. P.; Holms, J. H.; Young, P. R.; Carter, G. W. *J. Med. Chem.* **1988**, *31*, 1719.
35. Maga, G.; Falchi, F.; Radi, M.; Botta, L.; Casaluce, G.; Bernardini, M.; Irannejad, H.; Manetti, F.; Garbelli, A.; Samuele, A.; Zanoli, S.; Este, J. A.; Gonzalez, E.; Zucca, E.; Paolucci, S.; Baldanti, F.; DeRijck, J.; Debyser, Z.; Botta, M. *ChemMedChem* **2011**, *6*, 1371.
36. Homology model of LeuRS *Mycobacterium tuberculosis* was built using SWISS-MODEL workspace (http://swissmodel.expasy.org/).
37. Bursulaya, B. D.; Totrov, M.; Abagyan, R.; Brooks, C. L., III *J. Comput. Aided Mol. Des.* **2003**, *17*, 755.
38. Yakovenko, O. Ya.; Oliferenko, A. A.; Golub, A. G.; Bdzhola, V. G.; Yarmoluk, S. M. *Ukr. Bioorg. Acta* **2007**, *1*, 52.
39. Yakovenko, O. Ya.; Oliferenko, A. A.; Bdzhola, V. G.; Palyulin, V. A.; Zefirov, N. S. *J. Comput. Chem.* **2008**, *29*, 1332.
40. The structures were visualized using Discovery Studio Visualizer 4.0 (http://accelrys.com/).